

This article was downloaded by:

On: 21 January 2011

Access details: *Access Details: Free Access*

Publisher *Taylor & Francis*

Informa Ltd Registered in England and Wales Registered Number: 1072954 Registered office: Mortimer House, 37-41 Mortimer Street, London W1T 3JH, UK



International Journal of Polymer Analysis and Characterization

Publication details, including instructions for authors and subscription information:

<http://www.informaworld.com/smpp/title~content=t713646643>

A Recent Advance In The Application of Blending Laws in Mixed Biopolymer Systems

Ioannis S. Chronakis^a; Stefan Kasapis^a

^a Department of Food Research and Technology, Cranfield University, Silsoe College, Silsoe, Dedford, UK

To cite this Article Chronakis, Ioannis S. and Kasapis, Stefan(1995) 'A Recent Advance In The Application of Blending Laws in Mixed Biopolymer Systems', International Journal of Polymer Analysis and Characterization, 1: 2, 99 – 118

To link to this Article: DOI: 10.1080/10236669508233866

URL: <http://dx.doi.org/10.1080/10236669508233866>

PLEASE SCROLL DOWN FOR ARTICLE

Full terms and conditions of use: <http://www.informaworld.com/terms-and-conditions-of-access.pdf>

This article may be used for research, teaching and private study purposes. Any substantial or systematic reproduction, re-distribution, re-selling, loan or sub-licensing, systematic supply or distribution in any form to anyone is expressly forbidden.

The publisher does not give any warranty express or implied or make any representation that the contents will be complete or accurate or up to date. The accuracy of any instructions, formulae and drug doses should be independently verified with primary sources. The publisher shall not be liable for any loss, actions, claims, proceedings, demand or costs or damages whatsoever or howsoever caused arising directly or indirectly in connection with or arising out of the use of this material.

A Recent Advance In The Application of Blending Laws in Mixed Biopolymer Systems

IOANNIS S. CHRONAKIS AND STEFAN KASAPIS*

Department of Food Research and Technology, Cranfield University, Silsoe College, Silsoe, Bedford, MK45 4DT, UK

(Received September 20, 1993)

A survey of the literature clearly indicates the potential of steric exclusion phenomena between proteins and polysaccharides in enhancing the functional properties of food/non-food products. However, in spite of the range and depth of research over the last fifty years, even the most recent reviewers accept that there are still very significant areas of obscurity in our understanding of how phase-separated proteins and polysaccharides contribute to the texture of industrial products.

Recently, some progress has been made in the understanding of how biphasic gels behave in terms of phase continuity, phase inversion and, above all, solvent distribution between the two phases. It is based on the assumption that either bulk phase separation to equilibrium takes place first with gelation then occurring subsequently and independently in each phase or the fastest gelling component does so prior to the establishment of a true thermodynamic equilibrium with subsequent gelation of the second, slower gelling species. A number of theoretical treatments from the realm of synthetic polymers were adapted for use in biopolymer networks, namely: i) the application of blending laws to the phase separated biopolymer gels was attempted, taking into account the complication of solvent presence as a third component which can partition itself between the two polymer constituents, ii) the modulus development as a function of concentration (cascade formalism) was derived from the relationship between equilibrium shear modulus and number of elastically effective network chains considering that gel formation due to non-covalent interactions between biological macromolecules is described by a monomer-dimer equilibrium (link \leftrightarrow two free sites) and iii) the Flory de-swelling theory was applied to biopolymer gels assuming permanent networks on the basis of stress relaxation and dynamic oscillatory evidence. The conclusions, drawn from the theoretical postulates, were put to the test by acquiring independent evidence about the structural and mechanical properties of mixed gels using mechanical spectroscopy, differential scanning calorimetry, and microscopy. Studies were done using mixtures of several biopolymers (maltodextrins, gelatin, milk and soya proteins) in an attempt to identify a general pattern of behavior in the phase separation of biphasic gels. Overall, the analysis (theoretical model and experimental techniques) was extremely encouraging and the lack of direct (instrumental) determination of phase-composition makes it a most appropriate tool of attack for future research on biopolymer co-gels.

KEY WORDS Blending laws, cascade formalism, p parameter, thermodynamic equilibrium, de-swelling theory.

VISCOELASTIC BEHAVIOUR OF POLYMER BLENDS

In their classic work, Takayanagi, *et al.* [1] evaluated the viscoelastic behavior of polymer blends from the known properties of two component polymers. Accordingly, when the mutual miscibility of two polymers X and Y is very poor the

* To whom all correspondence should be addressed.

modulus of the composite (G_c) is calculated by assuming extreme cases in the distribution of strain and stress within the mixed system:

$$G_c = \phi_x G_x + \phi_y G_y \quad (1)$$

and

$$G_c = (\phi_x/G_x + \phi_y/G_y)^{-1} \quad (2)$$

where G_x and G_y are the shear moduli, with ϕ_x and ϕ_y ($\phi_x + \phi_y = 1$) being the phase volumes of the components X and Y , respectively. Equation (1) applies to isostrain conditions, where the continuous phase is more rigid than the disperse phase and the strain is uniform throughout the material (parallel model), whereas Equation (2) refers to isostress conditions, where the supporting phase is weaker than the discontinuous phase and both phases are now subjected to the same stress (series model). Obviously, when the continuous phase is stronger than the disperse phase, the composite modulus achieves a maximum value (upper bound behavior) whereas the system adopts a lower limit when the supporting phase is weaker than the discontinuous phase (lower bound behavior).

The above theory has successfully treated heterogeneous composites, where the elasticity of a chemically cross-linked component originates from the decrease in entropy of elastic chains due to a perturbation from the statistically most probable end-to-end distance [2]. Provided that the phase domains (i.e., ϕ_x and ϕ_y) are well defined, the equilibrium shear modulus (G_x or G_y) is derived by the Flory-Stockmayer random polycondensation model [3,4]:

$$G = \Phi N_e \quad (3)$$

where N_e is the number of elastically effective network chains ($EANCs$), formed through the covalent interaction of monomers with functionality f . At a temperature T , N_e depends on the degree of cross-linking of functionalities, α . When a network is just able to form, α is given by the following critical value [3]:

$$\alpha_c = 1/(f - 1) \quad (4)$$

Φ is a proportionality constant described by:

$$\Phi = gRT/V_{mol} \quad (5)$$

where RT is the entropy gain per mole of network chains in the strained polymer, V_{mol} is the volume per mole of repeat units, and g is a measure of the number of RT units contributed to the modulus by each mole of load-bearing chains in the network. In pure entropic networks (ideal rubbers) g takes the value of 1.

CONCENTRATION-DEPENDENCE OF MODULUS IN BIOPOLYMER GELS

The Effect of Extinction Probability on Network Connectivity

In the case of physically cross-linked biopolymer gels, elastic chains neither exhibit Gaussian (random-coil) behavior nor are linked together by point-like crosslinks.

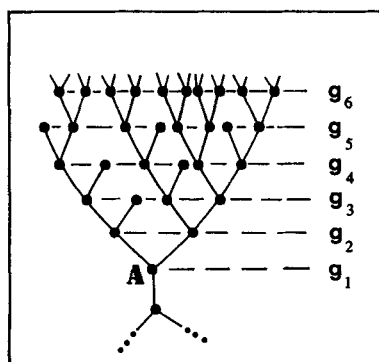


FIGURE 1 Schematic representation of a "subtree" within a polymer network. Values of g_n denote successive generations of constituent monomer units from the root at A . The "subtree" concept is used in the text to explain the definition of extinction probability, u (from reference 6, used with permission).

Instead, the major contribution to elasticity is attributed to the higher energy conformations of long junctions zones, occupying portions of the strained macromolecular chains. Clark and Ross-Murphy [5] accommodated the enthalpic nature of nonpermanent cross-links in the Flory-Stockmayer model by allowing the value of g to vary in Equation (5). Consequently, values of g much greater than unity were considered as evidence for non-rubberlike behavior in gelling biopolymers [5]. Furthermore, they realized that, unlike synthetic polymers where every covalent cross-link contributes to elastic phenomena, biopolymer systems contain a number of aggregates partially attached to the end of a network or single molecular "dangling ends" that are not capable of supporting stress. In view of that, they recalculated N_e , using the concept of extinction probability u within a biopolymer network. This is explained in Figure 1, using a trifunctional polycondensate network ($f = 3$) as an illustrative example [6]. The vertical bond linking the "subtree" rooted at point A to the rest of the network is termed extinct if the "subtree" is finite; if the "subtree" is infinite the linkage is termed a "tie". The "subtree" rooted at point A to the rest of the network is extinct, with probability u , if the two free functionalities pointing upward from A lead to finite subtrees (the third functional point is already used for the adherence of the trifunctional unit to the network). The chance $(1 - \alpha + \alpha u)$ that one of them creates a finite subtree is made up of two parts: a part $(1 - \alpha)$ that is found unreacted, which means immediate extinction, plus a chance αu that it has reacted to form a link which in turn leads only to a finite subtree. The chance that both available functionalities lead to extinction is thus:

$$u = (1 - \alpha + \alpha u)^2 \quad (6)$$

Removing of the obvious root ($u = 1$) and solving the resultant linear equation gives:

$$u = [(1 - \alpha)/\alpha]^2 \quad (7)$$

The extinction probability in the form of Equation (7) can be used for the derivation of the number N_e of *EANCs* per repeat unit. In the example of

trifunctional polycondensates this is equal to the number of active junction zones per repeat unit times $\frac{3}{2}$. Thus:

$$N_e = \frac{3}{2} [\alpha(1-u)]^3 = \frac{3}{2} [2\alpha - 1/\alpha]^3 \quad (8)$$

by using Equation (7). The factor $\frac{3}{2}$ occurs because each active junction point is here attached to three ties and each *EANC* is attached to two active junction points at its ends.

The generalization from a trifunctional system to one where the active junction points now have f ties used the general form of Equation (6):

$$u = (1 - \alpha + \alpha u)^{f-1} \quad (9)$$

in order to calculate the N_e as a function of both f and α [7]:

$$N_e = f\alpha(1-u)^2(1-b)/2 \quad (10)$$

where

$$b = (f-1)\alpha u / (1 - \alpha + \alpha u) \quad (11)$$

Substitution of Φ and N_e , as determined by Equations (5) and (10), respectively, into Equation (3) gives G as a function of α and f :

$$G = gRT \left[Nf\alpha(1-u)^2(1-b)/2 \right] \quad (12)$$

where N is the concentration of monomer species in moles per unit volume. The above equation constitutes the core of cascade formalism [8] and it has been used to define the mechanical characteristics of elastically active network chains of partially unfolded *BSA* molecules [9].

The Concept of Minimum Critical Gelling Concentration

Biopolymer networks not only waste a part of the physical cross-links in terms of enthalpic-elasticity behavior but they also rearrange the elastically active junction zones as a part of a thermodynamic equilibrium process (cross-link formation is opposed by bond breaking). Assuming that gel formation due to non-covalent interactions between macromolecules is described by a monomer-dimer equilibrium (link \leftrightarrow two free sites) and relating the modulus to concentration [10], the equilibrium constant for association is:

$$K = \alpha/NF(1-\alpha)^2 \quad (13)$$

N is readily estimated if the concentration c and the molecular weight M of the monomer are known:

$$N = c/M \quad (14)$$

Equation (13) can be solved for α , the result being:

$$\alpha = 1 + \left[\frac{1}{2}q \right] \left[1 - (4q + 1)^{1/2} \right] \quad (15)$$

where

$$q = NfK = fKc/M \quad (16)$$

by using Equation (14). As the course of association proceeds, there will be a critical degree of reaction where an effectively infinite network is formed. For a given temperature, this occurs at a minimum critical gelling concentration c_0 and the proportion of functional groups which has reacted is given by Equation (4). Substitution of α_c in Equation (15) allows the c_0 to be written in terms of f , K and M as

$$c_0 = M(f - 1)/Kf(f - 2)^2 \quad (17)$$

From the above equation, it is clear that for large f :

$$c_0 = M/Kf^2 \quad (18)$$

By combining Equations (12) with Equations (14) and (17) and collecting all terms together we have an expression for the shear modulus G :

$$GK/gRT = \{c/c_0\} \left\{ \left[(f - 1)\alpha(1 - u)^2(1 - b) \right] / \left[2(f - 2)^2 \right] \right\} \quad (19)$$

The above approach to biopolymer gelation takes into account the relationship between modulus development and extent of the reaction. It also predicts the commonly observed c_0 in gelling polysaccharides, which was not taken into consideration in earlier theories since the individual rheological properties of rubberlike material are independent of the macroscopic amount present. Subsequently, α depends only on f and the ratio of c/c_0 and thus Equation (19) defines the general concentration-dependence of G for a specific functionality, with differences in the molecular weight and equilibrium constant for junction formation in different polymer samples affecting only the scaling constants on either side of Equation (19). As a result, for each value of f , a universal "master curve" of G vs. c can be derived and the calculated moduli (at concentrations between or beyond those studied experimentally) may then be inserted in Equations (1) and (2) to estimate the equilibrium modulus of the composite (G_c).

SOLVENT DISTRIBUTION IN BIPHASIC BIOPOLYMER GELS

Phase Equilibrium vs. Kinetic Approach in Biopolymer Gelation

Having produced a cascade theory to calculate N_e , hence the molecular dependence of shear modulus in a biopolymer gel, we are almost ready to apply the blending laws in aqueous three-component systems. However, the inclusion of solvent (water) in the composite introduces one further complication that must be addressed first, namely: variable phase volumes (ϕ_x and ϕ_y), depending on the avidity of the two active gelling agents to attract water. Obviously, effective concentrations after phase separation are higher than the initial, nominal amounts

of the two polymer constituents and have to be estimated for use in the modulus-concentration relationship of Equation (19). Clark [11] tackled the problem of solvent partition by introducing the p parameter, the ratio of solvent to polymer in one phase divided by the corresponding ratio in the other phase:

$$p = (w_x/x)/(w_y/y) \quad (20)$$

Therefore, in a system where both the weights (x and y) of two polymers and water ($w = w_x + w_y$) are known, the p factor defines the phase volumes and hence the effective concentrations and real moduli of each biopolymer within its own phase. The above analysis was applied on composite agar-gelatin gels as follows: Experimental moduli were recorded for a series of mixed gels (holding the overall concentration of agar constant at 1 or 2% and varying the amount of gelatin in each agar series from 0 to 25%) and trial values of p were used to generate calculated upper and lower bound curves until a convincing fit was obtained [12]. Figure 2 shows the upper and lower bounds for the 1% agar gel series, assuming that the p factor equals 1. Upper and lower bound moduli (G_u and G_l) were calculated using the above approach [Equations (1) to (20)] and making the following two assumptions: i) bulk phase separation to thermodynamic equilibrium takes place first in solution with gelation then occurring subsequently and independently in each phase, and ii) the two polymers are confined entirely to their respective phases.

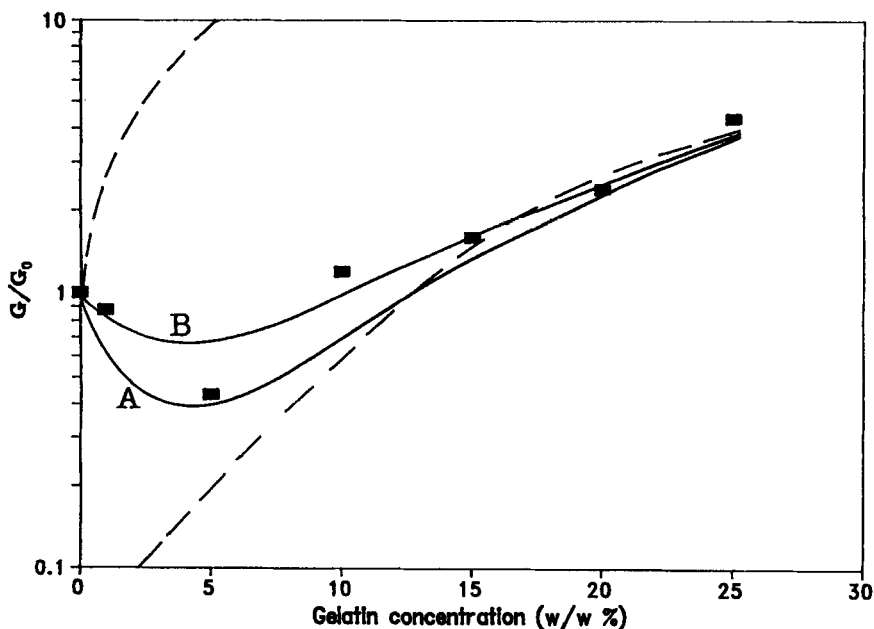


FIGURE 2 Shear modulus for the 1% agar series. Moduli are relative to the value for pure agar (G_0). Solid curves give the isostrain predictions for $p = 1$ and $q = 0.33$ (A) and 0.67 (B). Dashed lines show the upper and lower bounds for a phase separated system with labile cross-links at thermodynamic equilibrium (from reference 14, used with permission).

Alternatively, McEvoy *et al* [13,14]. argued that agar solutions during cooling set at higher temperatures than gelatin, effectively forming gels across the whole system at the nominal concentration (c^{nom}), of modulus G^{nom} . The agar network then is taken to a higher concentration (c^{eff}) of modulus G^{eff} by removal of water in a manner depending on the kinetics of subsequent gelatin gelation. In this process, the agar cross-links should be sufficiently labile and readjust to the new equilibrium condition in order the cascade fit to predict the concentration dependence of modulus. In view of the fact that agar networks remain effectively permanent within the conditions of the experiment (verified by dynamic oscillatory and tensile evidence [13]), the mechanical nature of a de-swelled agar network was described using the empirical formula [14]:

$$G^{\text{nom}}/G^{\text{eff}} = (c^{\text{nom}}/c^{\text{eff}})^{\sigma} \quad (21)$$

where the exponent σ was given values derived from entropically distorted materials, that is, $\frac{1}{3}$ for gels originally prepared as swollen networks [3] and $\frac{2}{3}$ in the case of cross-linked networks in solution [15]. The kinetic approach to agar-gelatin phase separation gave upper bounds (A and B in Figure 2) that reproduced the minimum in the experimental data at about 5% of gelatin in the mixed system. Overall the analysis (equilibrium and kinetic approach) represents a significant achievement, since it is the first time that the complicated mechanics of composite aqueous gels are rationalized with theories of polymer physics. However, there is still substantial scope for improvement as it is described in the following investigations.

Explicit Analysis of Solvent Partition and Polymer-Chain Contribution to Phase Volume in Gelling Biopolymer Blends

Recently the solvent partition approach was revived as a result of commercial interest in low-fat products where phase-separation phenomena between gelling biopolymers in the marketable product are of prime importance [16]. A new difficulty has arisen in these systems due to high overall polymer concentration. The earlier investigations [12,14] used dilute aqueous gels and thus assumed that the volume of polymer chains was negligible in comparison with the volume of the solvent. In the combinations studied lately, however, polymers constitute about a third of the total sample, so that their direct contribution to phase can no longer be ignored. Kasapis *et al.* [17] have tackled the problem by considering the following algorithm for each possible distribution of solvent between the component phases of mixed-gel combinations: the total weight of water in the system (w) can, of course, be calculated by subtracting the combined weights of the two polymers from the total weight. For each hypothetical partition of water between the two phases, S_x refers to the fraction of solvent in the polymer X phase and the weight of water in phases X and Y is then simply:

$$\begin{aligned} w_x &= S_x w \\ w_y &= (1 - S_x) w \end{aligned} \quad (22)$$

The total weights of the phases are then obtained by adding to the weight of the appropriate polymer:

$$\begin{aligned}tw_x &= x + w_x \\tw_y &= y + w_y\end{aligned}\tag{23}$$

Therefore, the effective concentrations (% w/w) of polymers X and Y in the two phases are:

$$\begin{aligned}c_x &= 100x/tw_x \\c_y &= 100y/tw_y\end{aligned}\tag{24}$$

To a good first approximation the total weights of the two phases then define the phase volumes [ϕ_x and ϕ_y in Equations (1) and (2)]. To obtain true phase volumes, however, the relative weights must be adjusted for density differences between the phases. Since the correction is a minor one, the concentration-dependence of gel density for the two polymers was calibrated by the rather crude (but rapid) procedure of filling a pre-weighed measuring cylinder with the appropriate solution, allowing the gel to form, reading off its volume, and determining its density from the final weight. The results obtained for a few concentrations of each polymer yielded the following relationship between polymer concentration c and relative density D ;

$$\begin{aligned}D_x &= 1.0 + Rc_x \\D_y &= 1.0 + Rc_y\end{aligned}\tag{25}$$

where R is a concentration coefficient particular to the experimental system. Having taken into account the density differences between the two phases, the relative volumes of regions X and Y are:

$$\begin{aligned}V_x &= tw_x/D_x \\V_y &= tw_y/D_y\end{aligned}\tag{26}$$

Finally the phase volumes in the composite can be written in terms of the relative volumes as:

$$\begin{aligned}\phi_x &= V_x/(V_x + V_y) \\ \phi_y &= V_y/(V_x + V_y)\end{aligned}\tag{27}$$

The values of phase volumes can be used directly in Equations (1) and (2), alongside the calculated moduli of the individual components at their effective concentrations (cascade treatise), for derivation of shear modulus of the composite (G_u and G_1).

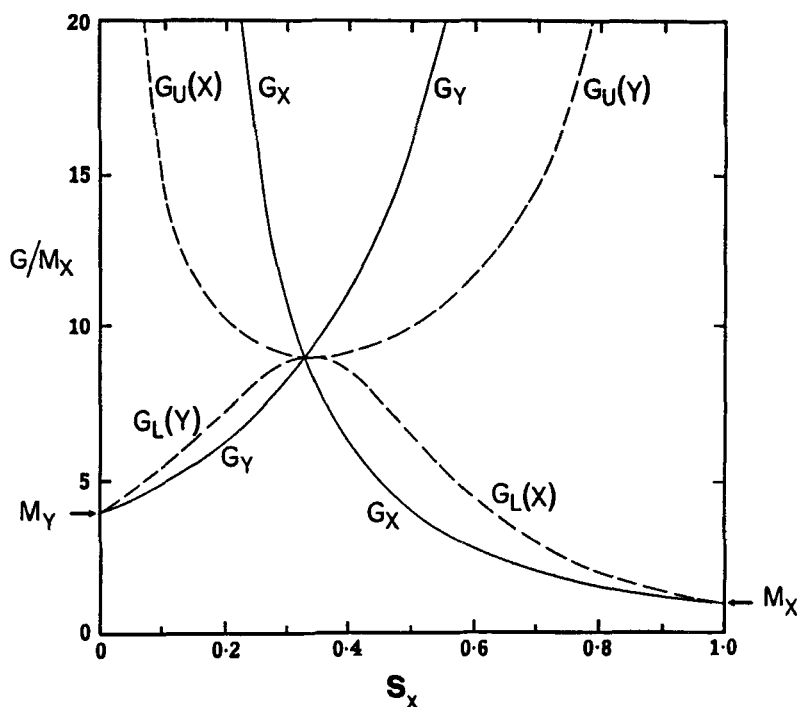


FIGURE 3 Effect of solvent fraction in the polymer X phase (S_x) on the value of calculated moduli (G/M_x). At their nominal concentrations, polymer Y is four times stronger than X ($M_y = 4M_x$). Solid lines trace the variation in network strength of the individual components (G_x and G_y), whereas broken lines represent the shear moduli of the composite according to isostrain and isostress model (G_u and G_l respectively). In both cases the continuous network is shown in brackets (from reference 18, used with permission).

Figure 3 [18] demonstrates the computerized output derived for a phase-separated mixed gel of two polymers, X and Y , which at their nominal concentrations across the whole system would have moduli M_x and M_y , respectively, with: $M_y = \Delta M_x$ (in this example, Δ is assumed to have the value of 4). Variation in calculated moduli is plotted against S_x . As the value of S_x increases from 0 to 1, the calculated values of G_x decrease whereas those of G_y increase. A point is reached where the solvent partition between the biopolymers is such that the two curves cross, making identical the rigidity of the phases. At the same time the upper bound (X -continuous phase; isostrain conditions) descends from the top-left corner of the diagram, with the lower bound (Y -continuous phase; isostress conditions) rising from the bottom-left one, meeting again at the same "critical" point. Beyond this common point the physical significance of the bounds swaps over, with the Y -continuous phase representing the upper bound (isostrain conditions) and with converse significance for the X -continuous phase (lower bound; isostress conditions). If the identity of the continuous phase is known from comparison of melting profiles of single component and mixed gels (see Figure 6) it should then be possible to determine the precise value of S_x (and hence of p) required to give perfect agreement with the observed modulus for a specific binary gel.

QUANTITATIVE ANALYSIS OF BIOPOLYMER MIXED GELS MODULI

Theoretical and Experimental Characterization of Mixed Gels Structure

The theoretical model and working assumptions, evolved in Equations (1) to (27) were put to the test in several biphasic gels. Figure 4 shows the family of bounds obtained for a mixed system of highly hydrolyzed potato starch (maltodextrin of dextrose equivalent about 4) from Cerestar address in the covering letter and a

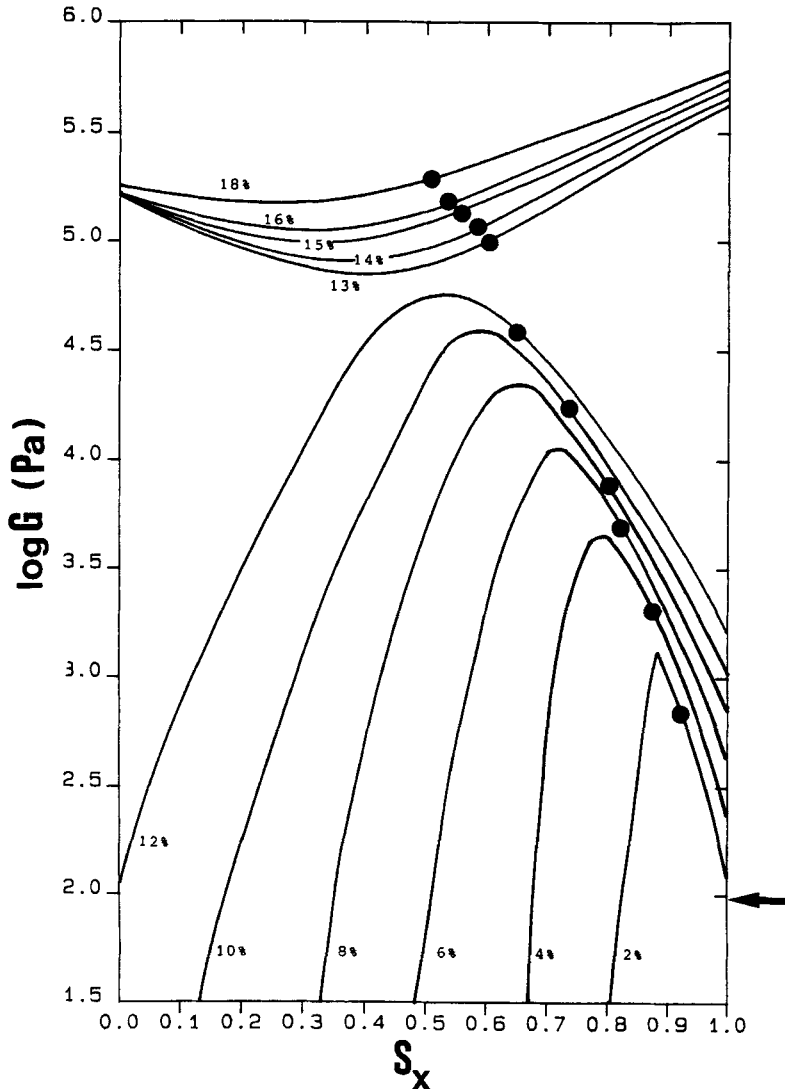


FIGURE 4 Calculated bounds for the mixed gels of 16.5% w/w milk protein series as a function of solvent fraction in the Promilk phase (S_x). In the milk protein continuous systems (2 to 12% maltodextrin in the composite) only the lower bounds are drawn whereas at maltodextrin concentrations beyond the inversion point (13 to 18%) the isostrain predictions are illustrated. Experimental values are shown to intercept the bounds and the experimental modulus for 16.5% milk protein in isolation is noted by the arrow on the right-hand axis [25].

commercial milk protein supplied by Ingredia address in the covering letter (Promilk). In this treatment, the Promilk protein is regarded as polymer X at a constant concentration of 16.5% throughout, so that the parameter S_x refers to the fraction of solvent in the milk protein phase whereas the amount of maltodextrin (polymer Y) varies between 2 and 18%. Results are based on the theoretical postulate that gelation of both components occurs at their final concentrations in their respective phases as materialized in the cascade formalism of Equation (19). Overall, the phase equilibrium analysis of solvent-partition between the two components suggests a phase inversion from a weak, continuous matrix (lower bound; isostress conditions) to a strong, supporting network (upper bound; isostrain conditions) at $12.5 \pm 0.5\%$ of maltodextrin. For reasons of clarity, only the lower bounds are illustrated in Figure 4 for combinations below the phase inversion point and *vice versa*.

To test the validity of the theoretical analysis in terms of phase inversion and to identify the phase separated microstructure as roughly spherical inclusions of maltodextrin embedded in a milk protein matrix, or *vice versa*, a sequel of experimental approaches is invoked. First, mixed systems are prepared by combining appropriate amounts of individual stock solutions held in a stable form at 45°C. Upon mixing the protein and maltodextrin, solutions become cloudy, indicating that they consist of phase-separated droplets large enough to scatter visible light. On centrifugation, the opaque solutions separate into two liquid layers, the lower one consisting predominantly of milk protein and the top one being rich in maltodextrin. Second, the thermal changes accompanying gel melting of the individual components is characterized by differential scanning calorimetry (DSC).

Figure 5a shows the endotherm observed on melting of a 18% w/w maltodextrin gel, with a transition mid-point temperature (T_m) value of about 72°C. On the contrary, the DSC trace of milk protein (16.5% w/w) is a monotonic line (Figure 5b), since the production of Promilk involves spray drying ($\approx 80^\circ\text{C}$) causing thermally irreversible protein denaturation (absence of any further micromolecular conformational transitions on subsequent reheating of the polymer in the calorimeter). The corresponding melting profiles (obtained under identical experimental conditions) for mixed gels of 16.5% w/w milk protein with 6 and 18% w/w maltodextrin are reproduced in Figures 5c and d. These combinations correspond to maltodextrin concentrations well below and well above the critical value of about 12.5% w/w at which the transition from the isostress to isostrain conditions is observed in the theoretical analysis (Figure 4). In both cases the thermograms show traces that correspond closely in position and general band-form to those of the individual components in isolation. The obvious conclusion from this evidence is that there are no specific interactions between the two components, that is, no formation of heterotypic junctions that produce their own network and thus distort the temperature characteristics of the endothermic process (the curve for the mixture shows two peaks), as it has been observed for a number of cooperative, mixed gels [19,20].

The temperature-course of gel melting is monitored by mechanical spectroscopy. Figure 6a shows two typical melting profiles of milk protein (22.5%) and maltodextrin (21%). Clearly, there is a substantial difference in the melting behavior of the two polymers, with the milk protein gels melting out completely at

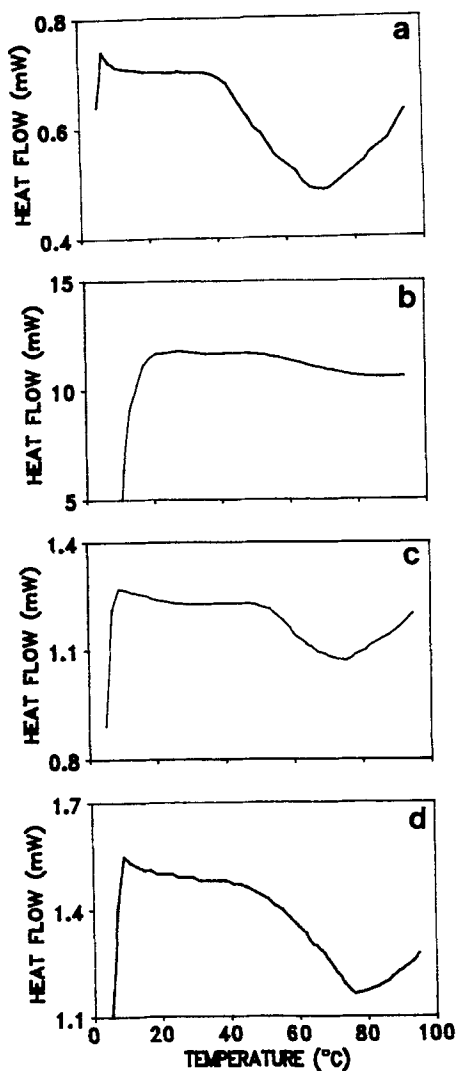


FIGURE 5 Melting endotherms from DSC heating scans (5–95°C; 0.1 deg/min) for a) 18% maltodextrin; b) 16.5% milk protein; c) 16.5% milk protein + 6% maltodextrin; and d) 16.5% milk protein + 18% maltodextrin [25].

temperatures above 60°C, whereas the maltodextrin gels maintain significant structure up to 80°C. As shown in Figure 6b the melting behavior of mixed gels follows two discrete patterns. At the lower range of maltodextrin concentrations (2–12%) in the mixed system, networks melt out completely over the temperature range of the mechanical collapse of the individual milk protein gels (i.e., at about 60°C; illustrated typically for the 16.5% milk protein and 8% maltodextrin sample), whereas at higher content of maltodextrin (13–18%) melting of the protein component is accompanied by a reduction in moduli but the gel remains intact until the higher temperature range associated with melting of the individual maltodextrin networks (i.e., at about 80°C; e.g., in the case of 16.5% milk protein and 18% maltodextrin composite). The overriding conclusion to be drawn from

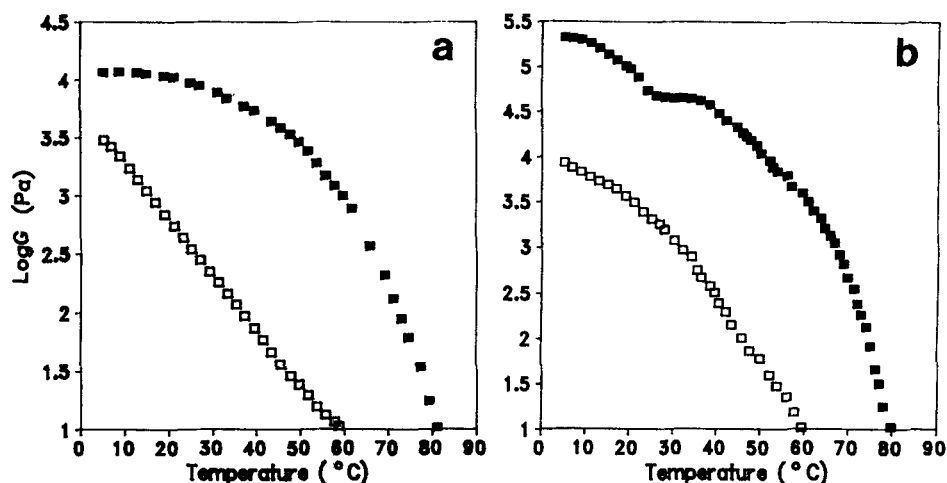


FIGURE 6 a) Temperature-dependence of G on thermal melting of 22.5% milk protein (□) and 21% maltodextrin (■) gels set at 5°C for 90 minutes; b) Gel melting for 16.5% milk protein-8% maltodextrin (□) and 16.5% milk protein-18% maltodextrin (■). Conditions as before [25].

Figures 4, 6a, and 6b is that phase inversion from a weak and continuous milk protein network with strong maltodextrin inclusions to a network in which maltodextrin forms the supporting and strong phase, with milk protein dispersed as the discrete and more deformable particles of microgel, occurs at maltodextrin concentration in the composite of about 12.5%.

Experimental Derivation of the p Factor in Phase Equilibria Analysis

Up to this point, the physical properties of component phases and the composite system itself have comprehensively identified. The last requirement in maltodextrin-Promilk mixed gels is to rationalize the manner in which the two polymers partition the available solvent. This is readily achieved with the estimation of p parameter, which is neither anticipated nor assumed, but emerges directly from the analysis. Combining Equations (20) and (22), a direct relation between solvent fraction, S_x and solvent avidity parameter, p is derived:

$$p = (S_x/x)/([1 - S_x]/y) \quad (28)$$

A trivial modification in the computerized algorithm allows the calculated bounds of Figure 4, to be displayed as a function of p . When the experimental moduli of the mixed systems, already presented in Figure 4, are replotted in this way (Figure 7), it is clear that the intercepts in the milk protein continuous systems produce a single value of p about 1.7 ($\log p \approx 0.23$), whereas the data beyond the phase inversion point (maltodextrin continuous system) are better fitted with a value of p about 1.1 ($\log p \approx 0.04$).

Another protein-polysaccharide system where the applicability of p parameter was investigated included two different types of potato maltodextrin (Paselli SA-2 and SA-6 with dextrose equivalent values of 2 and 6 respectively) from Avebe addresses in the covering letter and a second extract limed-ossein gelatin (LO-2)

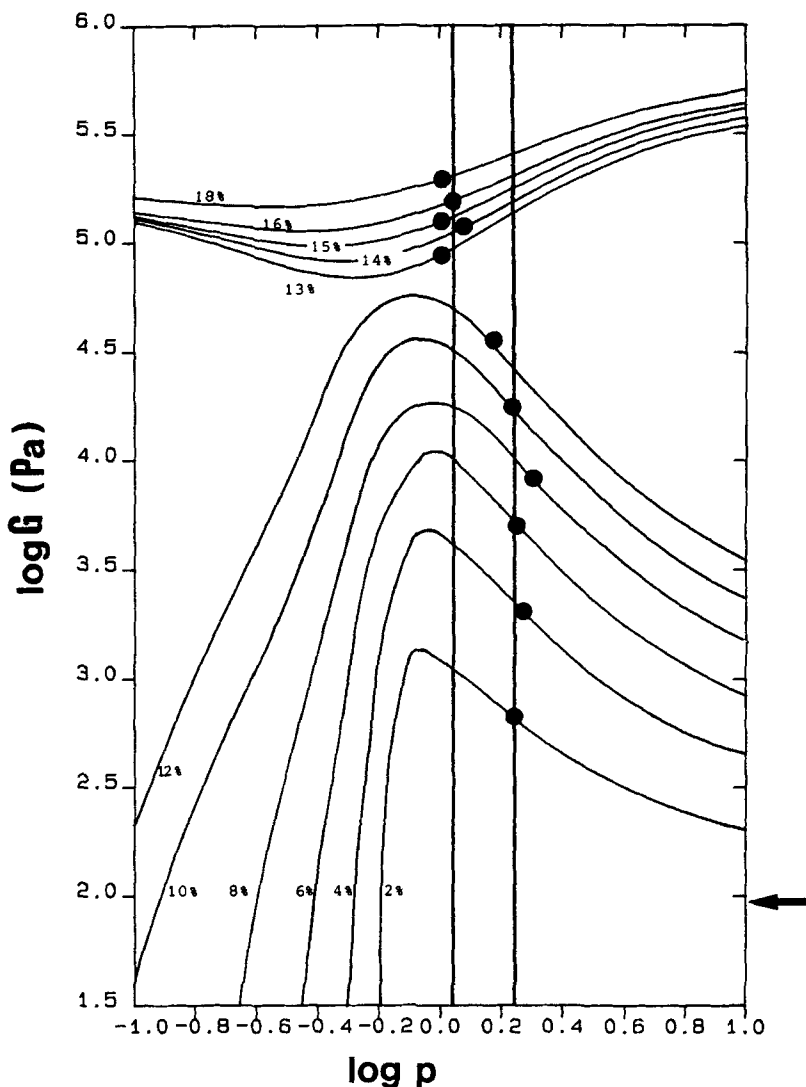


FIGURE 7 Calculated lower or upper bounds for 16.5% milk protein with maltodextrin at concentrations (% w/w) show, plotted as a function of the solvent-avidity parameter, p . Symbols as in Figure 4 [25].

from Sanofi. Meeting the requirements of the analysis, every effort was made to document that single component gels of SA-2, SA-6 and LO-2 form effectively permanent networks [21], that binary systems are of the phase separated type [22] and that mixed gels phase invert from a gelatin continuous matrix to a microstructure where maltodextrin is the supporting phase [23]. At the end, the shear modulus of biphasic gels was quantitatively related to the experimentally determined concentration dependence of G for the constituent polymers thus allowing the prediction of solvent distribution between the component phases. For more than 30 combinations of maltodextrin-gelatin mixed gels, good agreement with the experimental data was achieved for a single value of $p \approx 1.8$ [17].

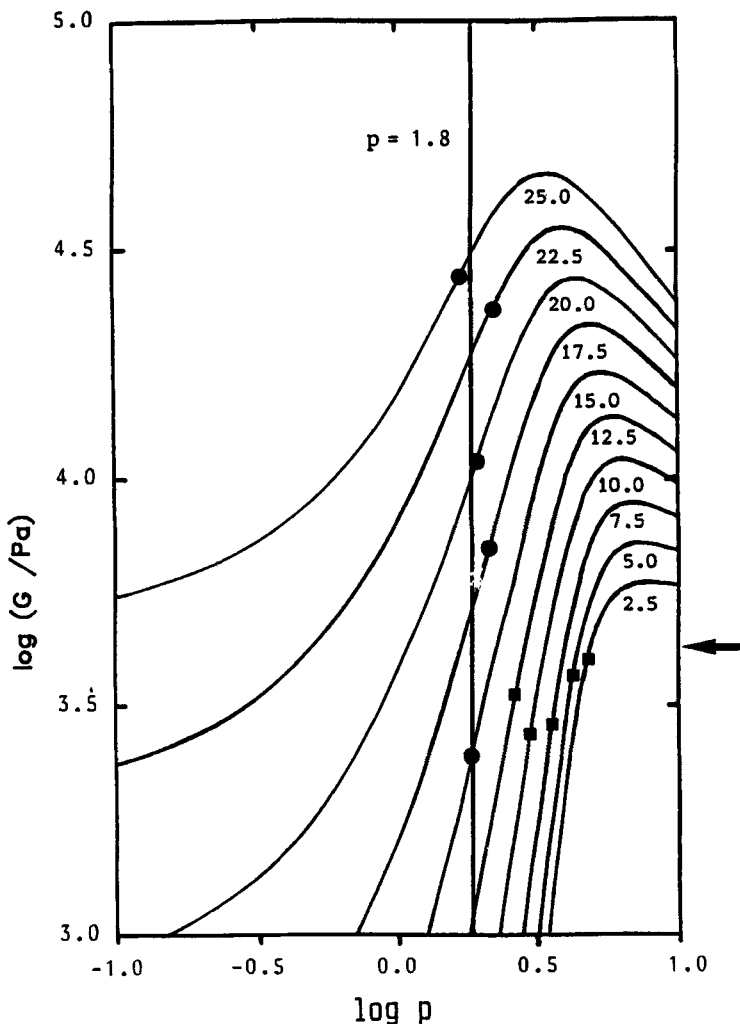


FIGURE 8 Calculated lower bounds for 5% w/w LO-2 with SA-6 at the concentrations (% w/w) shown, plotted as a function of solvent avidity parameter, p . Experimental values are shown on the maltodextrin continuous bound for physically realistic (●) and physically unrealistic (■) situations. The experimental modulus for 5% LO-2 in isolation is shown by the arrow on the right-hand axis (from reference 17, used with permission).

Figure 8 presents the sensitivity of the model to the value of p on the 5% gelatin series (2.5 to 25% SA-6), where only the calculated lower bounds are plotted for clarity. As expected, beyond the phase inversion point ($14 \pm 1\%$ maltodextrin in this series) results are resolved at the p value of 1.8. However, at composite combinations where gelatin is the continuous phase (2.5 to 13% SA-6) results remain close or fall below the gelatin modulus at nominal concentration (5%), rendering unsuitable the theoretical postulate of thermodynamic equilibrium between the component phases [cascade fit of Equation (19)]. Instead, this pattern of behavior is explained on the basis of de-swelling theory [Equation (21)], assuming that the faster-gelling species, gelatin, does so at its original concentra-

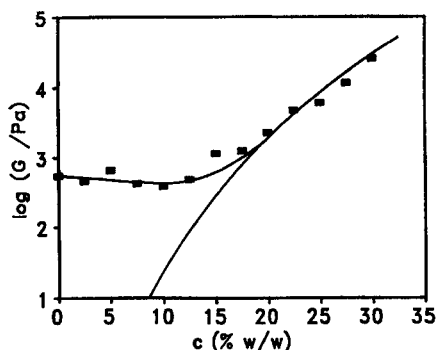


FIGURE 9 Comparison of experimental moduli for mixed gels of 2% w/w LO-2 with varying concentrations of SA-6. In this gelatin series, phase inversion occurs at about 17.5% w/w of SA-6. The steep line shows the calculated moduli for a maltodextrin continuous network formed at its final concentration. The shallow curve corresponds to a gelatin continuous network formed at its nominal concentration, with subsequent deswelling (from reference 17, used with permission).

tion throughout the system, followed by gelation of maltodextrin that claims some of the solvent from the gelatin network. The shallow curve in Figure 9 demonstrates the standard of agreement achieved between experimental points of the composite gels and expected moduli, calculated on the basis of initial gelation and subsequent de-swelling of gelatin. In doing so, the p value was held constant at 1.8 and the swelling factor, σ , was taken at the theoretical value for a permanent network ($\sigma = \frac{2}{3}$). Finally, the steep line in Figure 9 shows the calculated moduli for a maltodextrin continuous network beyond the phase inversion point, formed at its final concentration (treatment analogous to that in Figure 8).

The maltodextrin-gelatin studies have emphasized that the relationship between modulus development and time is of vital importance in understanding the structural properties of phase-separated gels. The kinetic approach to explicit analysis of water partition between two de-mixed polymers was thus pursued by using cold-setting aqueous preparations of thermally processed milk (Promilk) and soya (commercially available as Supro 760 from Protein Technologies International address in the covering letter) proteins [24]. Mechanical characterization of individual samples has shown similar properties in terms of thermally induced rates of gelation, concentration dependence of pseudo-equilibrium modulus above 20% polymer, terminal relaxation times in simple compression, and pattern of failure under large deformation analysis.

A possible interpretation of this behavior might be that the thermal processing caused extensive denaturation to the protein molecules which in the hydration state form roughly spherical colloidal clusterings of comparable functionality. Obviously there is a straightforward positive relationship between "performance" characteristics of the protein network and polymer density in the system that can be used to manipulate the rheological behavior and water immobilization of one gelling agent on the expense of the other. Figure 10 demonstrates the application of de-swelling theory to milk protein continuous networks (10%) with soya inclusions as the discontinuous phase (6 to 16%). When the experimental data are plotted on the calculated bounds, physically realistic results are obtained for the

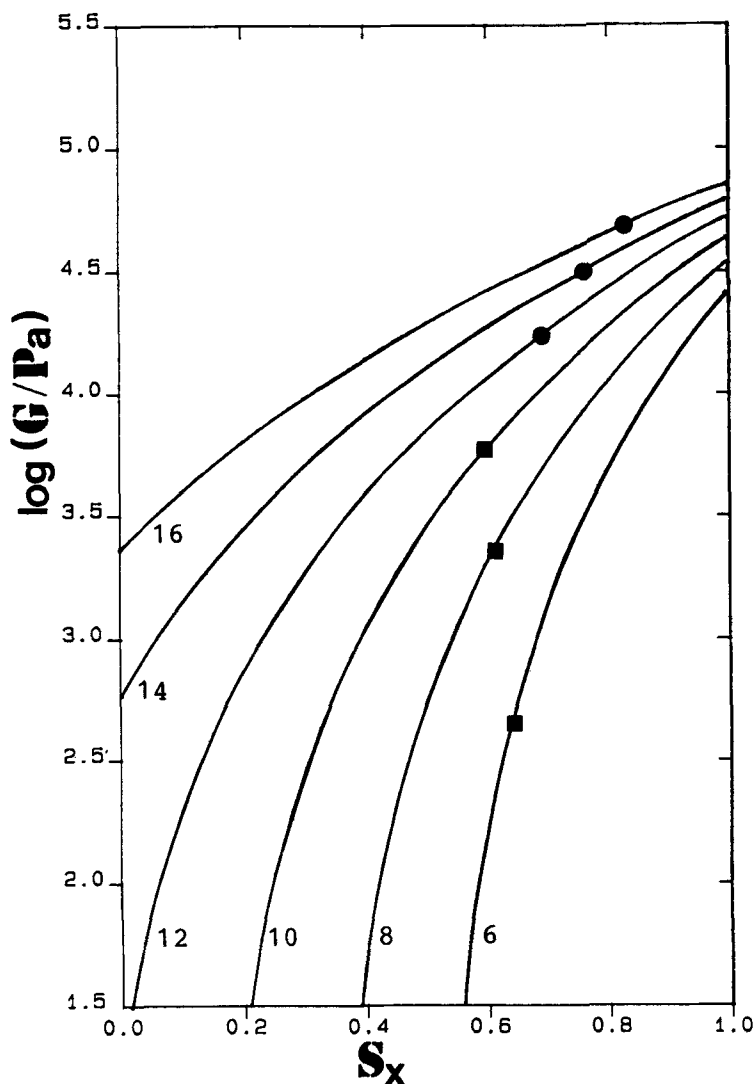


FIGURE 10 Calculated Promilk continuous bounds for 10% milk protein with soya protein at concentrations (% w/w) shown. Experimental values are shown on the Promilk continuous bound for physically realistic (■) and physically unrealistic (●) situations (from reference 24, used with permission).

soya concentration range of 6 to 10%, as expected from the concentration advantage of the milk protein component. Beyond that, the composite systems are entirely unrealistic since the milk phase seems to be capable of binding more of the available solvent at higher concentrations of soya protein. Molecular interactions in the upper half of the composite combinations (12 to 16% soya protein) are described, however, by means of the phase equilibria model, yielding a soya continuous network with a water to polymer ratio 1.25 times (p value) higher than in the milk protein phase. Overall, theoretical considerations and experimental

evidence argue that phase inversion from a milk protein continuous network to a system where soya protein forms the supporting matrix, occurs at a soya concentration of about 11%.

CONCLUSION

The application of physical theories from the realm of synthetic polymers to gelation and phase separation of biopolymer systems has been reviewed. Discussion on composite gels was by no means exhaustive, but rather it reflects the personal biases of the authors. It is clear, however, that the framework of the analysis pursued is based on simple, well-understood kinetic-thermodynamic considerations. Thus it is reasonable to assume that thermodynamic incompatibility between the disordered chains of maltodextrin and the thermally unfolded globular protein molecules promotes an early phase separation, as described in the elaborate treatment of Figure 4. However, conformationally similar species like the disordered coils of maltodextrin and gelatin or the globular structures of milk and soya macromolecules might tolerate each other at low concentrations in a monophasic solution. During subsequent cold-setting, the faster-gelling polymer could develop its network prior to the establishment of micro-phase separation that awaits gelation of the second species. This idea was successful in modeling the lower range of concentrations in the gelatin and milk protein series (Figures 9 and 10, respectively), where the aforementioned biopolymers are believed to employ faster rates of gelation than their counterparts. However, in both systems, at combinations above the phase inversion point, it seems that the kinetic effect is swamped by the enthalpic disadvantage in polymer segments being surrounded by others of a different type. As a result, classic phase separation might occur, requiring the quantitative analysis of modulus *versus* composition behavior of the cascade model. The interplay of kinetic and thermodynamic forces has been also observed in phase-separation studies of gelatin and maltodextrin systems in solution, [22] that is, combinations above 2% LO-2 and 20% SA-6 resolve into two co-existing liquid layers, whereas at lower concentrations maltodextrin chains, in the presence of disordered gelatin coils, aggregate and then form a precipitated gel.

Since in phase-separated gels, the partition of solvent between polymers characterizes their mechanical properties, accurate estimation of the p parameter becomes an important aspect of the analysis. The p parameter is a simple way of describing the solvent distribution between two co-existing polymer phases. Characterization of modulus *versus* composition data in agar-gelatin mixed gels was based on the assumption that the p value was independent of concentration. It is doubtful, however, that the solvent avidity of two polymers X and Y remains unaffected by changes in the gelling conditions from a reference state. Figure 7 illustrates two distinct families of p values, surrounding the transition from isostress to isostrain conditions in the milk protein-maltodextrin composite system. Furthermore, within each type of filled network, there is no systematic variation of p with polymer concentration. A simple explanation of this behavior is that the water binding capacity is not only a reflection of the individual properties of a

polymer but it also depends on the geometrical organization of the composite's microstructure. Obviously, by accepting diffusion to osmotic equilibrium as the mechanism behind water rearrangement, the approximately round-shaped filler would expose relatively less surface for a given volume, thus reducing its "intrinsic" relative power of attraction for solvent.

The slow rate of water diffusion between the solid-like phases in a composite gel makes it necessary to apply the p factor concept only in the case of complete de-mixing, that is, when a true phase equilibrium has been achieved. In a phase-separated system under kinetic control it is meaningless to invoke a p factor since evolving conformational changes, chain aggregation, and water redistribution are time-related processes. Single-point observations do not necessarily reflect the eventual avidity of two polymer constituents for water. Keeping this in mind, Kasapis *et al.* [17,21–24] assessed the small deformation properties of de-swelled gelatin gels on the basis that the kinetically controlled sequence of gel formation reached thermodynamic equilibrium after 7 h of experimentation (Figure 9). In the case of milk-soya protein mixed systems this approach was not followed since the solvent diffusion between the two phases was found to be very slow (the system reached a thermodynamically stable state at the end of a three-week period). In general, the authors believe that the p and q factors should not be used indiscriminately in systems under kinetic control since there is a time constraint attached to this process.

Finally, comparison of the maltodextrin continuous networks in Figures 7 and 8 reveals that the model is also sensitive to changes in rigidity of the supporting phase. According to Equations (1) and (2) the mechanical properties of a composite material are mainly those of the continuous network, altered in a consistent manner by the presence of filler (isostrain or isostress conditions). Therefore, in the case of Paselli maltodextrin-gelatin mixed gels, where the moduli of individual gels are of comparable magnitude [21] a weaker maltodextrin continuous phase surrounding stronger beads of gelatin (isostress case in Figure 8) is well accepted from the standpoint of the Takayanagi theory. Conversely, the overall rigidity of a composite network might be relatively insensitive to a weak filler when the moduli of the two components differ significantly. This is illustrated in Figure 7 (isostrain conditions), where gels of the Cerestar maltodextrin are about one and a half orders of magnitude stronger than those of the milk protein [25].

Acknowledgments

The authors wish to thank Professor E. R. Morris and Dr. R. K. Richardson, Cranfield University/UK for helpful discussions.

References

1. M. Takayanagi, H. Harima, and Y. Iwata, *Mem. Fac. Eng. Kyushu Univ.*, **23**, 1, (1963).
2. J. A. Manson and L. H. Sperling, *Polymer Blends and Composites* (Heyden Press, London, 1976).
3. P. J. Flory, *Principles of Polymer Chemistry* (Cornell University Press, New York, 1953), pp. 348 and 576.

4. W. H. Stockmayer, *J. Chem. Phys.*, **11**, 45 (1943).
5. A. H. Clark and S. B. Ross-Murphy, *Brit. Pol. J.*, **17** (1985).
6. M. Gordon and S. B. Ross-Murphy, *Pure Appl. Chem.*, **43**, 1 (1975).
7. G. R. Dobson and M. Gordon, *J. Chem. Phys.*, **43**, 705 (1965).
8. M. Cordon, *Proc. Roy. Soc. (London) Ser. A*, **268**, 240 (1962).
9. R. K. Richardson and S. B. Ross-Murphy, *Int. J. Biol. Macromol.*, **3**, 315 (1981).
10. J. R. Hermans, *J. Polym. Sci. A*, **3**, 1859 (1965).
11. A. H. Clark, *Food Structure and Behaviour*, J. M. V. Blanshard and P. Lillford, eds. (Academic Press, London, 1987), p. 13.
12. A. H. Clark, R. K. Richardson, S. B. Ross-Murphy and J. M. Stubbs, *Macromol.*, **16**, 1367 (1983).
13. H. McEvoy, S. B. Ross-Murphy and A. H. Clark, *Polymer*, **26**, 1483 (1985).
14. H. McEvoy, S. B. Ross-Murphy and A. H. Clark, *Polymer*, **26**, 1493 (1985).
15. R. E. Cohen, S. D. Severson, C. U. Yu, and J. E. Mark, *Macromol.*, **10**, 663 (1977).
16. P. Mageean and S. Jones, *Food Science & Technology Today*, **3**, 162 (1989).
17. S. Kasapis, E. R. Morris, I. T. Norton, and A. H. Clark, *Carbohydr. Polym.*, **21**, Part IV, 269 (1993).
18. E. R. Morris, *Carbohydrate Polymers*, **17**, 65 (1992).
19. P. A. Williams, D. H. Day, M. J. Langdon, G. O. Phillips, and K. Nishinari, *Food Hydrocolloids*, **4**, 489 (1991).
20. P. A. Williams, S. M. Clegg, M. J. Langdon, K. Nishinari, and G. O. Phillips, *Gums and Stabilisers for the Food Industry 6*, G. O. Phillips, P. A. Williams and D. J. Wedlock, eds. (IRL Press, Oxford, 1991), p. 209.
21. S. Kasapis, E. R. Morris, I. T. Norton, and A. H. Clark, *Carbohydr. Polym.*, **21**, Part I, 243 (1993).
22. S. Kasapis, E. R. Morris, I. T. Norton, and M. J. Gidley, *Carbohydr. Polym.*, **21**, Part II, 249 (1993).
23. S. Kasapis, E. R. Morris, I. T. Norton, and C. R. T. Brown, *Carbohydr. Polym.*, **21**, Part III, 261 (1993).
24. I. S. Chronakis and S. Kasapis, *Food Hydrocolloids*, **7**, 459 (1993).
25. I. S. Chronakis and S. Kasapis, unpublished results.